

Original Article



OPEN ACCESS

Received: Oct 13, 2022

Revised: Jan 15, 2023

Accepted: Jan 28, 2023

Published online: Feb 3, 2013

Correspondence to

Duk Lyul Na

Department of Neurology, Samsung Medical Center, Sungkyunkwan University School of Medicine, 81 Irwon-ro, Gangnam-gu, Seoul 06351, Korea.

Email: dukna@naver.com

© 2023 Korean Dementia Association

This is an Open Access article distributed under the terms of the Creative Commons Attribution Non-Commercial License (<https://creativecommons.org/licenses/by-nc/4.0/>) which permits unrestricted non-commercial use, distribution, and reproduction in any medium, provided the original work is properly cited.

ORCID iDs

Young Hee Jung

<https://orcid.org/0000-0002-8945-2200>

Seongbeom Park

<https://orcid.org/0000-0002-0759-6826>

Na Kyung Lee

<https://orcid.org/0000-0001-6116-2562>

Hyun Jeong Han

<https://orcid.org/0000-0002-1129-6340>

Hyemin Jang

<https://orcid.org/0000-0003-3152-1274>

Hee Jin Kim

<https://orcid.org/0000-0002-3186-9441>

Sang Won Seo

<https://orcid.org/0000-0002-8747-0122>

Duk Lyul Na

<https://orcid.org/0000-0002-0098-7592>

White Matter Lesions Predominantly Located in Deep White Matter Represent Embolic Etiology Rather Than Small Vessel Disease

Young Hee Jung ¹, Seongbeom Park ², Na Kyung Lee ^{2,3,4}, Hyun Jeong Han ¹, Hyemin Jang ^{2,4}, Hee Jin Kim ^{2,3,4,5}, Sang Won Seo ^{2,4,5,6,7}, Duk Lyul Na ^{2,3,4,6}

¹Department of Neurology, Myoungji Hospital, College of Medicine, Hanyang University, Goyang, Korea

²Department of Neurology, Samsung Medical Center, Sungkyunkwan University School of Medicine, Seoul, Korea

³Stem Cell & Regenerative Sciences and Technology, SAIHST, Sungkyunkwan University, Seoul, Korea

⁴Alzheimer's Disease Convergence Research Center, Samsung Medical Center, Seoul, Korea

⁵Department of Digital Health, SAIHST, Sungkyunkwan University, Seoul, Korea

⁶Department of Health Science and Technology, SAIHST, Sungkyunkwan University, Seoul, Korea

⁷Department of Intelligent Precision Healthcare Convergence, Sungkyunkwan University, Suwon, Korea

ABSTRACT

Background and Purpose: We investigated the correlation between the deep distribution of white matter hyperintensity (WMH) (dWMH: WMH in deep and corticomedullary areas, with minimal periventricular WMH) and a positive agitated saline contrast echocardiography result.

Methods: We retrospectively recruited participants with comprehensive dementia evaluations, an agitated saline study, and brain imaging. The participants were classified into two groups according to WMH-distributions: dWMH and dpWMH (mainly periventricular WMH with or without deep WMH.) We hypothesized that dWMH is more likely associated with embolism, whereas dpWMH is associated with small-vessel diseases. We compared the clinical characteristics, WMH-distributions, and positive rate of agitated saline studies between the two groups.

Results: Among 90 participants, 27 and 12 met the dWMH and dpWMH criteria, respectively. The dWMH-group was younger (62.2 ± 7.5 vs. 78.9 ± 7.3 , $p < 0.001$) and had a lower prevalence of hypertension (29.6% vs. 75%, $p = 0.008$), diabetes mellitus (3.7% vs. 25%, $p = 0.043$), and hyperlipidemia (33.3% vs. 83.3%, $p = 0.043$) than the dpWMH-group. Regarding deep white matter lesions, the number of small lesions (<3 mm) was higher in the dWMH-group (10.9 ± 9.7) than in the dpWMH-group (3.1 ± 6.4) ($p = 0.008$), and WMH was predominantly distributed in the border-zones and corticomedullary areas. Most importantly, the positive agitated saline study rate was higher in the dWMH-group than in the dpWMH-group (81.5% vs. 33.3%, $p = 0.003$).

Conclusions: The dWMH-group with younger participants had fewer cardiovascular risk factors, showed more border-zone-distributions, and had a higher agitated saline test positivity rate than the dpWMH-group, indicating that corticomedullary or deep WMH-distribution with minimal periventricular WMH suggests embolic etiologies.

Keywords: Cerebrovascular Disorder Patent Foramen Ovale; Embolism

Funding

This work was supported by a fund from Research of Korea Centers for Disease Control and Prevention (2021ER100500).

Conflict of Interest

The authors have no financial conflicts of interest.

Author Contributions

Conceptualization: Park S, Na DL; Data curation: Jung YH; Formal analysis: Jung YH; Investigation: Jung YH, Na DL; Methodology: Jung YH; Project administration: Jung YH; Resources: Jung YH; Supervision: Han HJ, Kim HJ, Seo SW, Na DL; Validation: Jung YH, Na DL; Visualization: Jung YH, Park S; Writing - original draft: Jung YH, Na DL; Writing - review & editing: Jung YH, Lee NK, Jang H, Na DL.

INTRODUCTION

Cerebral small vessel disease (CSVD) affects the small arteries, arterioles, venules, and capillaries in the brain (size ranging from 3 to 100 μm).^{1,2} CSVD cannot be identified solely by magnetic resonance (MR) angiography. Instead, white matter hyperintensity (WMH) and other CSVD magnetic resonance imaging (MRI) markers, such as lacunes, microbleeds, and perivascular spaces, serve as surrogate markers. WMH can lead to subcortical vascular cognitive impairment, which consists of mild subcortical vascular cognitive impairment and subcortical vascular dementia.³ However, individuals with WMH are generally asymptomatic despite the presence of severe WMH and other CSVD markers. WMH can also result from a variety of etiologies other than CSVD, including radiation injury, multiple sclerosis, and leukodystrophy.⁴ Alzheimer's pathology often coexists in CSVD patients, increasing the complexity of CSVD, and can be identified via amyloid positron emission tomography (PET).^{5,6} A previous study from our group suggested that younger CSVD patients had a higher likelihood of obtaining negative amyloid PET scans if an increase in the number of lacunes and reduced medial temporal atrophy (MTA) were evident.⁷ Therefore, in this present study, we defined the dpWMH group as individuals with significant WMH, at least one lacune, and absent or mild MTA, regardless of their cognitive status. Individuals with dpWMH have both periventricular and deep WMH, which is considered to be associated with CSVD.

However, we often encounter individuals in the clinic with WMH lesions whose patterns are different from those of the dpWMH group. As exemplified in **Fig. 1** and **Supplementary Fig. 1**, the WMH lesions in these patients are mainly located in the corticomedullary junction or deep white matter, accompanied by no or minimal WMH lesions contiguous to the lateral ventricles. Specifically, WMH can be classified into deep and periventricular WMH in terms of location. Periventricular WMH is contiguous with the margin of each lateral ventricle and usually manifests as a cap or band. Deep WMH lesions are patchy and congruent and are separate from the lateral ventricles, usually more than 10 mm from the surface of the ventricle.⁸ Unlike individuals with dpWMH, who usually have both deep and periventricular WMH, we defined the dWMH group as individuals with WMH lesions that were mainly located in the corticomedullary junction or deep white matter, accompanied by little, if any, periventricular WMH. This deep WMH pattern (dWMH) has not been systematically studied, especially its etiology.⁹

We hypothesized that the underlying etiology of dWMH might be due to an embolism of cardiac or extracardiac origin. The WMH lesions in the dWMH group tended to be mainly located in the corticomedullary and border zone areas, which is similar to the WMH distribution seen in patients with a high risk of paroxysmal embolism due to patent foramen ovale (PFO), one of the most common causes of cardiac embolism.^{10,11} In addition, patients in the dWMH group often present with a few vascular risk factors, such as hypertension, diabetes mellitus (DM), or hyperlipidemia, which is also characteristic of those with a high risk of paroxysmal embolism.¹² Therefore, our hypothesis originated from the observation that the dWMH group and patients with a high risk of paradoxical embolism had WMH distribution and clinical characteristics in common.¹²

In the current study, we performed agitated saline contrast echocardiography in both the dpWMH and dWMH groups and examined whether the two groups differed in shunt frequency.

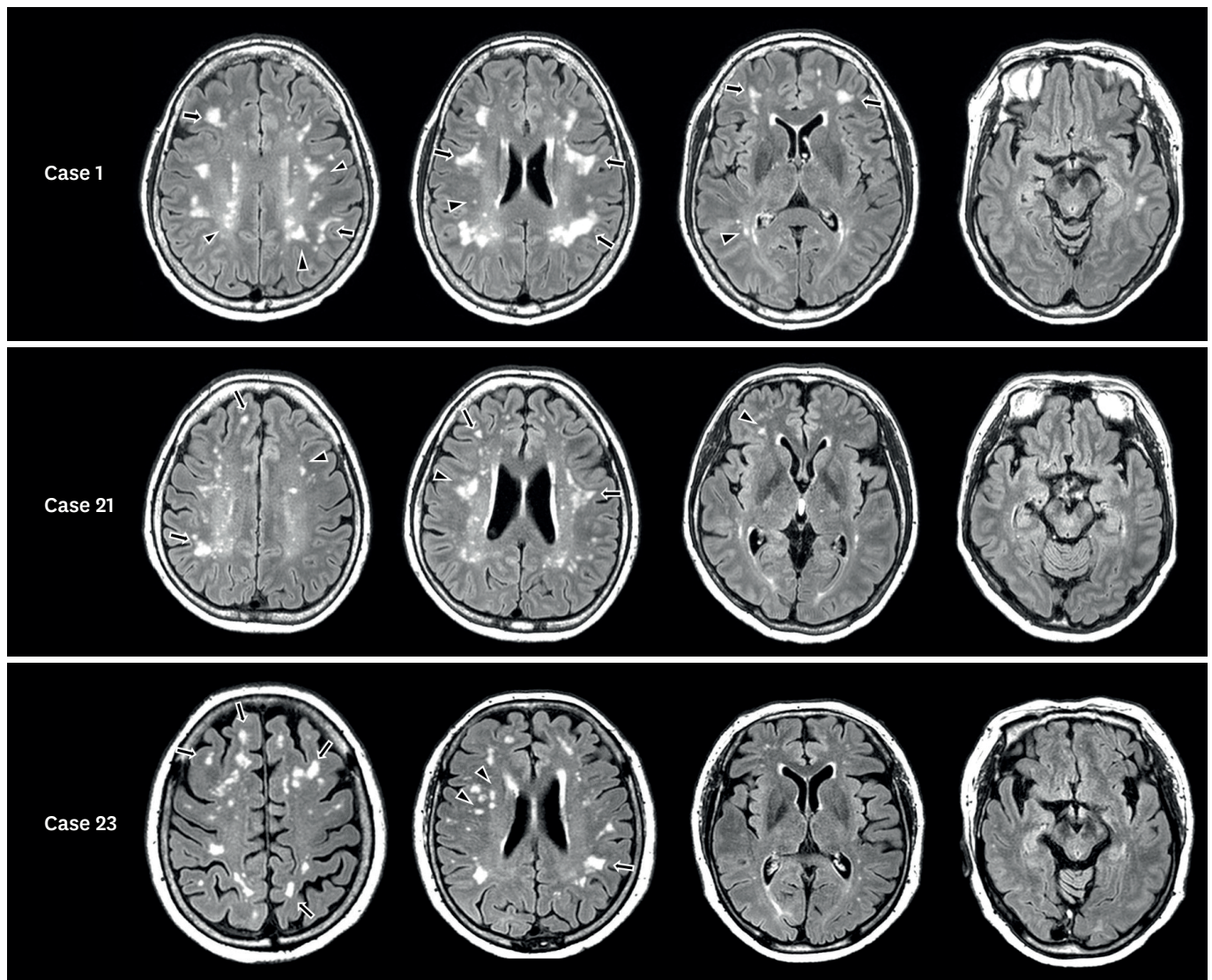


Fig. 1. Distribution of white matter lesions in representative cases in the dWMH group. FLAIR images of the dWMH group show small, scattered white matter hyperintense lesions in the deep white matter (arrowheads) and corticomedullary junction (tailed arrows). dWMH: deep-only WMH pattern in which WMHs are mainly located in the corticomedullary junction or deep white matter, accompanied by little or no periventricular WMH, dpWMH: WMH pattern that is commonly seen in individuals with cerebral small vessel disease, where main periventricular WMH with or without deep WMH is accompanied by one or more lacunes, WMH: white matter hyperintensity.

METHODS

Standard protocol approvals, registration, and patient consent

The Institutional Review Board of Myongji Hospital approved this study protocol, and the requirement for written informed consent was waived as the study was retrospective. All procedures were performed in accordance with approved guidelines.

Study participants and definitions of the dWMH and dpWMH groups

We retrospectively identified 90 patients recruited between May 2016 and April 2019 from the Memory Disorder Clinic at Myongji Hospital. These patients underwent comprehensive dementia evaluations, agitated saline contrast echocardiography, and brain MRI. Of these

90 patients, 19 patients were excluded for the following reasons: 1) the presence of WMH lesions associated with etiologies other than CSVD, such as radiation injury, leukodystrophy, multiple sclerosis, and other autoimmune encephalopathies; 2) the detection of intra/extracranial artery stenoses on brain MR angiography; 3) history of cardiac diseases that could cause embolism, such as atrial fibrillation; and 4) meeting the Boston Criteria for cerebral amyloid angiopathy (CAA).¹³

Those in the dWMH group met the following criteria: 1) WMH mainly located in the deep white matter and corticomedullary junction based on FLAIR images; 2) the presence of minimal periventricular WMH <P2 (caps ≤ 5 mm or band ≤ 5 mm)¹⁴ and no lacunes; and 3) MTA grade 2 or less on Scheltens' visual rating scale.⁷ Second, we classified individuals with typical CSVD into the dpWMH group, which satisfied the following criteria in the same study period: 1) significant periventricular WMH (caps ≥ 10 mm and band ≥ 10 mm),¹⁴ 2) at least one lacune, and 3) MTA grade 2 or less on Scheltens' visual rating scale.⁷

Dementia evaluation

The participants underwent a comprehensive dementia evaluation that included history taking, neurological examination, blood tests to exclude secondary dementia causes, brain MRI, and cognitive assessments, including the Mini-mental Status Examination (MMSE), Seoul Neuropsychological Screening Battery, and Clinical Dementia Rating-sum of the boxes. This evaluation helped to identify the underlying causes of cognitive impairment and classify the participants into either of the following categories: subjective cognitive decline, mild cognitive impairment, or dementia.^{15,16}

Agitated saline contrast echocardiography (agitated saline study)

Two-dimensional echocardiography was performed using commercially available equipment (Vivid 7; GE Medical Systems, Milwaukee, WI, USA). In the apical four-chamber view, the left-to-right shunt at the atrial level was evaluated using color flow Doppler. A right-to-left intra-atrial shunt was evaluated by contrast injection (10 mL of agitated saline) at rest and by the Valsalva maneuver (VM). To investigate the presence of an extracardiac shunt, the contrast agent injection was performed when the pulmonary vein was open.¹⁷ The direct passage from the right atrium to the left atrium across the interatrial septum or the early appearance of bubbles in the left atrium (within three to five beats) after right chamber opacification during rest or VM suggests an intracardiac shunt. The later appearance of bubbles in the left atrium (>5 beats after first observing bubbles in the right atrium) suggests pulmonary arteriovenous shunting.¹⁸

A positive shunt test was achieved when at least one definite microbubble was observed in the left chamber.¹⁹⁻²¹ The amount of right-to-left shunt (RLS) was semi-quantified as follows: grade 0 (no microbubbles), grade I (1–5 microbubbles), grade II (6–20 microbubbles), grade III (21–50 microbubbles), and grade IV (>50 microbubbles). Grade I or II was considered small RLS, and grade III or IV indicated large RLS, adopted from the grading system used for R-L shunt.¹⁹⁻²¹

Brain MRI acquisition

MR images from all participants were obtained using an Achieva 3.0 T MRI scanner (Philips, Best, The Netherlands), which included FLAIR and T2*GRE from all participants. The following parameters were used for the FLAIR images: axial slice thickness, 2 mm; no gap, TR of 11,000 ms; TE, 125 ms; flip angle, 90°; and matrix size, 512×512 pixels. The following parameters were used for the T2*GRE images: axial slice thickness, 5.0 mm; inter-slice thickness, 2 mm; repetition time, 669 ms; echo time, 16 ms; flip angle, 18°; and matrix size, 560×560 pixels.

WMH assessment

WMH lesion assessment was performed by two experienced neurologists who were trained in neuroimaging rating and blinded to the participants' clinical details. WMH lesions were rated on a visual rating scale proposed by the Clinical Research Center for Dementia of South Korea (CREDOS).¹⁴ Deep WMH was classified as D1 (<10 mm), D2 (10–25 mm), or D3 (\geq 25 mm) based on the longest diameter of the lesions. Periventricular WMH were classified as P1 (caps and band <5 mm), P2 (5–10 mm), or P3 (cap or band \geq 10 mm) based on the maximum length measured perpendicular (cap) and horizontal (band) to the ventricle.^{3,14} We assessed WMH lesions on every other FLAIR image as the images were acquired without a gap and at a thickness of 2 mm.

We only counted WMH lesions where the longest diameter was longer than 2 mm because exceedingly small, unspecified bright objects (UBOs) are considered normal, and small UBOs can be a manifestation of small perivascular spaces (<2 mm), which have been regarded as anatomic variations.^{22–25} In terms of WMH distribution, periventricular lesions were defined as those located within 10 mm from the ventricular surface,⁸ corticomedullary lesions as those within 4 mm from the corticomedullary junction,²⁶ and deep white matter lesions as those between the periventricular and corticomedullary junction areas.²⁶

Confluent periventricular WMH lesions were excluded from the number of WMH lesions. Each isolated WMH lesion in the deep and corticomedullary regions, was counted as a single lesion, even if partially confluent. The size of each lesion was determined by its longest diameter.

Assessment of lacunes and microbleeds

Lacunes were counted in accordance with the standards for reporting vascular changes on neuroimaging.²⁷ Lacunes were defined as round or ovoid, subcortical, fluid-filled cavities (signal similar to cerebrospinal fluid) between 3 mm to about 15 mm in diameter, consistent with a previous acute small subcortical infarct or hemorrhage in the territory of one perforating arteriole according to STRIVE guidelines.²⁸ Considering that our FLAIR images were obtained at a thickness of 2 mm and no gap, we counted the number of lacunes on every other FLAIR image.

Microbleeds were defined as homogenous, round lesions displaying a signal loss (\leq 10 mm in diameter) in T2*GRE images.²⁹ Considering that our GRE images were obtained with a thickness of 5 mm and a 2 mm gap, we counted the number of microbleeds on every other GRE image.

Visual rating of medial temporal lobe atrophy

Medial temporal lobe atrophy (MTA) was assessed visually by an experienced neurologist.³⁰ The degree of MTA was rated from 0 (no atrophy) to 4 (severe atrophy). If it was asymmetric between the left and right, the more severe MTA was selected for the patient.

Image creation to compare WMH distribution between the dpWMH and dWMH groups

WMH lesions on each FLAIR-MRI slice were manually marked using MRICro software to create a composite image of WMH spatial distribution. The T2*FLAIR-MRI images were co-registered to each individual's 3D T1 MR images, which were then registered to the Montreal Neurological Institute's 152 templates. We then applied normalized parameters to transform the co-registered T2*FLAIR MRIs using the MRI template. The manually marked lesions were subsequently re-sampled into the template space (**Fig. 2**).

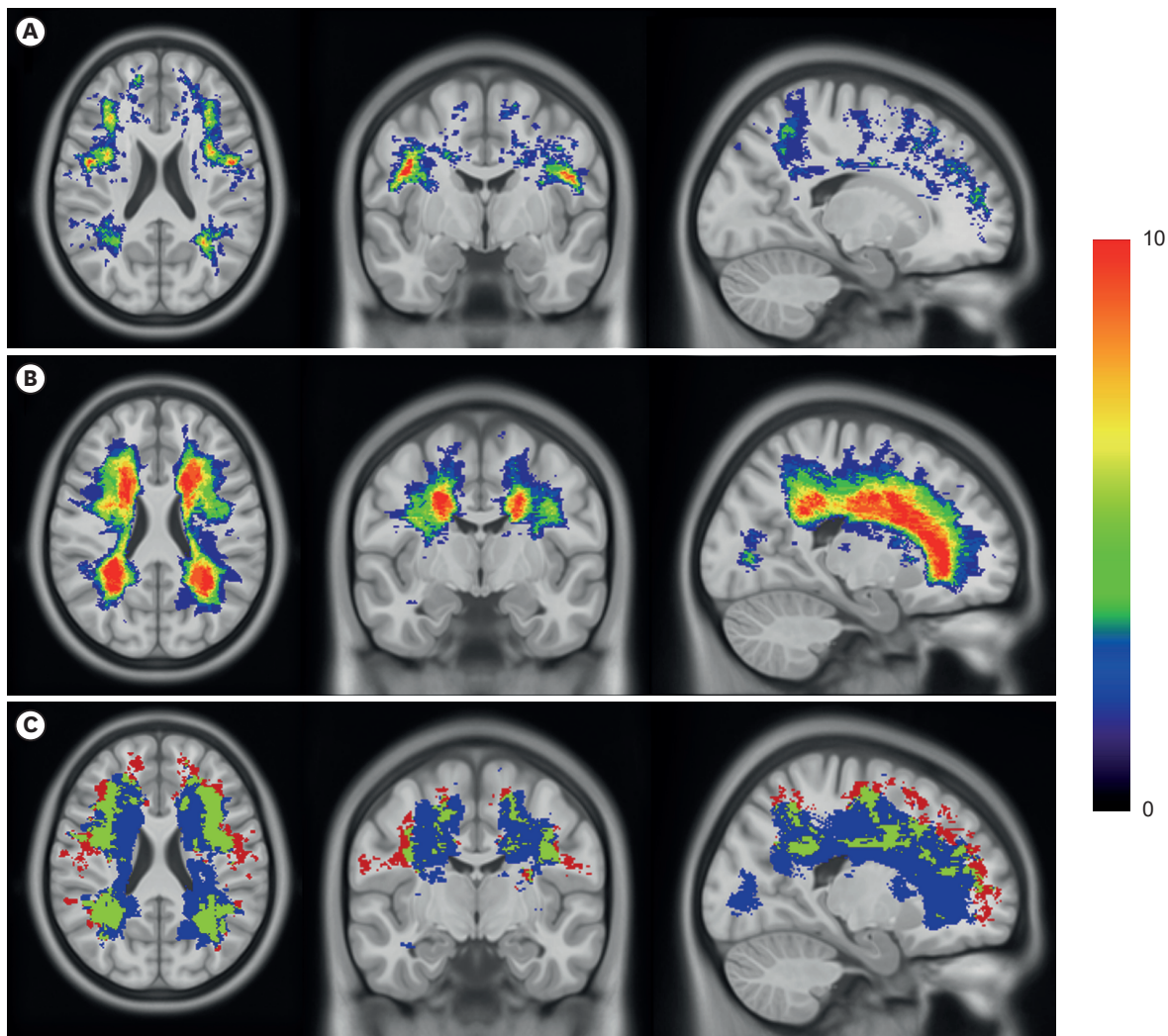


Fig. 2. Comparison of WMH distribution between the dWMH and the dpWMH groups. WMH lesions were manually cropped from the patients' FLAIR slices using MRlcro, co-registered to 3D T1 images, and superimposed onto MNI templates (see Methods for details). (A, B) WMH lesions from a patient in the dWMH (A) and the dpWMH (B) group were superimposed onto MNI templates. The red and blue colors indicate higher and lower frequencies, respectively, as indicated by the color bar on the far right. (C) Spatial distribution of the WMH lesions evident in both dWMH and dpWMH groups (red: WMH lesions shown exclusively in the dWMH group, blue: WMH lesions shown exclusively in the dpWMH group, green: lesions overlapping in both groups).

WMH: white matter hyperintensity, dWMH: deep-only WMH pattern in which WMHs are mainly located in the corticomedullary junction or deep white matter, accompanied by little or no periventricular WMH, dpWMH: WMH pattern that is commonly seen in individuals with cerebral small vessel disease, where main periventricular WMH with or without deep WMH is accompanied by one or more lacunes.

Statistical analyses

For descriptive statistics, we used the χ^2 test and Student's *t*-test to compare the clinical/imaging characteristics and shunt frequency between the groups. Post-hoc analysis was performed after pooling the dWMH and dpWMH groups. Linear regression was used to determine the association between age and the presence of cardiovascular factors.

Statistical significance was set at a two-tailed *p*-value of <0.05 . Statistical analyses were conducted using the Statistical Package for the Social Sciences software version 25 (SPSS Inc., IBM Corp., Armonk, NY, USA).

Data availability

Data that support the findings of this study will be made available by the corresponding author upon reasonable request.

RESULTS

Demographic characteristics

After excluding 19 of the initial 90 according to the exclusion criteria, 39 of the remaining 71 patients met either the dWMH (27/39) or the dpWMH (12/39) criteria. Of the 39 patients, 27 were classified into the dWMH group, and 12 were classified into the dpWMH group (Table 1). Overall, the dWMH group was younger than the dpWMH group (62.2±7.5 vs. 78.9±7.3 years,

Table 1. Demographic data of the study participants

| Variables | dWMH group (n=27) | dpWMH group (n=12) | p-value |
|---------------------------------|-------------------|--------------------|---------|
| Age | 62.2±7.5 | 78.7±7.3 | <0.001 |
| Female | 21/27 (77.8) | 8/12 (66.7) | 0.463 |
| Hypertension | 8/27 (29.6) | 9/12 (75) | 0.008 |
| Diabetes mellitus | 1/27 (3.7) | 3/12 (25) | 0.043 |
| Hyperlipidemia | 9/27 (33.3) | 10/12 (83.3) | 0.016 |
| The number of lacunes | 0 | 3.3±2.5 | 0.001 |
| Prevalence of TIA/CVA | 0 (0) | 1/12 (8.3) | 0.129 |
| Cognitive status | | | <0.001 |
| SCD | 17/27 (65.4) | 1/12 (8.3) | |
| MCI | 9/27 (34.6) | 5/12 (41.7) | |
| Dementia | 0 (0) | 6/12 (50.5) | |
| MMSE | 25 (28.8±1.9) | 25.0±3.9 | <0.001 |
| CDR | 25 (0.5±0.1) | 0.7±0.5 | 0.015 |
| CDR-SOB | 25 (0.9±0.8) | 3.0±3.3 | 0.005 |
| Variables | dWMH group (n=27) | dpWMH group (n=12) | p-value |
| No. of total WMH lesions | 155.6±82.3 | 53.3±53.1 | <0.001 |
| Longest diameter of WMH (mm) | 14.7±8.1 | 52.5±14.8 | <0.001 |
| Anatomical distribution of WMH | | | |
| Deep WM lesion (total) | 31.1±34.4 | 27.6±20.7 | 0.695 |
| <3 mm | 10.9±9.7 | 3.1±6.4 | 0.008 |
| 3–10 mm | 17.3±24.4 | 15.6±11.9 | 0.776 |
| 10–20 mm | 2.5±7.2 | 6.0±5.4 | 0.114 |
| >20 mm | 0.4±1.8 | 5.4±4.0 | 0.002 |
| Corticomedullary lesions, total | 124.5±75.6 | 25.7±40.9 | <0.001 |
| <3 mm | 60.3±48.3 | 7.1±14.4 | <0.001 |
| 3–10 mm | 59.4±41.2 | 16.6±25.6 | 0.001 |
| 10–20 mm | 4.2±9.9 | 2.4±4.0 | 0.416 |
| >20 mm | 0.7±2.6 | 1.9±3.3 | 0.284 |
| Variables | dWMH group (n=27) | dpWMH group (n=12) | p-value |
| Saline shunt test | 22/27 (81.5) | 4/12 (33.3) | 0.003 |
| Intracardiac shunt | 18/22 (81.8) | 2/4 (50.0) | |
| Extracardiac shunt | 4/22 (18.2) | 2/4 (50.0) | |
| Shunt grade | 1.8±1.2 | 0.5±0.9 | 0.003 |
| 0 | 5 (18.5) | 8 (66.7) | |
| I | 4 (14.8) | 1 (8.3) | |
| II | 12 (44.4) | 3 (25) | |
| III | 4 (14.8) | 0 (0) | |
| IV | 2 (7.4) | 0 (0) | |

Values are presented as mean ± standard deviation or number (%).

dWMH: deep-only WMH pattern in which WMHs are mainly located in the corticomedullary junction or deep white matter, accompanied by little or no periventricular WMH, dpWMH: WMH pattern that is commonly seen in individuals with cerebral small vessel disease, where main periventricular WMH with or without deep WMH is accompanied by one or more lacunes, TIA: transient ischemic attack, CVA: cerebral vascular accident, SCD: subjective cognitive decline, MCI: mild cognitive disorder, MMSE: Mini-mental Status Examination, CDR-SOB: Clinical Dementia Rating-sum of the boxes, WMH: white matter hyperintensity.

$p < 0.001$). Compared to the dWMH group, the dpWMH group showed a higher prevalence of hypertension (29.6% vs. 75%, $p = 0.008$), DM (3.7% vs. 25%, $p = 0.043$), and hyperlipidemia (33.3% vs. 83.3%, $p = 0.043$). The participants in the dWMH group (28.8 ± 1.9) showed higher MMSE scores than those in the dpWMH group (25.0 ± 3.9) ($p < 0.001$).

In the post-hoc analysis using linear regression, after pooling the dWMH and dpWMH groups, younger age was correlated with a lower presence of cardiovascular factors ($R^2 = 0.370$, $B = 0.10$, $p < 0.001$).

Comparison of WMH burden and distribution between groups

The total number of WMH lesions was higher in the dWMH group (155.7 ± 82.3) than in the dpWMH group (53.3 ± 53.1) ($p < 0.001$). The diameter of the largest lesion was larger in the dpWMH (52.5 ± 14.8) group than in the dWMH group (14.7 ± 8.1) ($p < 0.001$) (**Table 2**).

In terms of deep WMH, the number of small lesions (< 3 mm) was higher in the dWMH group (10.9 ± 9.7) than in the dpWMH group (3.1 ± 6.4) ($p = 0.008$), whereas the number of large lesions (> 20 mm) was lower in the dWMH group (0.4 ± 1.8) than in the dpWMH group (5.4 ± 4.0) ($p = 0.002$).

The total number of corticomedullary lesions was higher in the dWMH group (124.5 ± 75.6) than in the dpWMH group (25.7 ± 40.9) ($p < 0.001$). In particular, the number of small lesions (< 10 mm) was higher in the dWMH group than in the dpWMH group (< 3 mm: 59.4 ± 41.2 vs. 16.6 ± 25.6 , $p < 0.001$; 3 mm – 10 mm: 59.4 ± 41.2 vs. 16.6 ± 25.6 , $p = 0.001$) (**Table 2** and **Fig. 3**).

As shown in **Fig. 2A**, WMH lesions in the dWMH group were located between the territories of the anterior cerebral artery (ACA), middle cerebral artery (MCA), and posterior cerebral artery (PCA) (external border zone) or in the white matter along and slightly above the lateral ventricle, between the deep and superficial arterial systems of the MCA, or between the superficial systems of the MCA and ACA (internal border zone). The frequency map revealed that the WMH lesions in the dpWMH group were predominantly located in the periventricular area, followed by the contiguous deep white matter area (**Fig. 2B**). The WMH distribution in the two groups showed distinct patterns, although they partly overlapped (**Fig. 2C**).

Table 2. Characteristics and distribution of WMH between the groups

| Variables | dWMH group (n=27) | dpWMH group (n=12) | p-value |
|---------------------------------|-------------------|--------------------|---------|
| No. of total WMH lesions | 155.6±82.3 | 53.3±53.1 | <0.001 |
| Longest diameter of WMH (mm) | 14.7±8.1 | 52.5±14.8 | <0.001 |
| Anatomical distribution of WMH | | | |
| Deep WM lesion (total) | 31.1±34.4 | 27.6±20.7 | 0.695 |
| <3 mm | 10.9±9.7 | 3.1±6.4 | 0.008 |
| 3–10 mm | 17.3±24.4 | 15.6±11.9 | 0.776 |
| 10–20 mm | 2.5±7.2 | 6.0±5.4 | 0.114 |
| >20 mm | 0.4±1.8 | 5.4±4.0 | 0.002 |
| Corticomedullary lesions, total | 124.5±75.6 | 25.7±40.9 | <0.001 |
| <3 mm | 60.3±48.3 | 7.1±14.4 | <0.001 |
| 3–10 mm | 59.4±41.2 | 16.6±25.6 | 0.001 |
| 10–20 mm | 4.2±9.9 | 2.4±4.0 | 0.416 |
| >20 mm | 0.7±2.6 | 1.9±3.3 | 0.284 |

Values are presented as mean ± standard deviation.

WMH: white matter hyperintensity, dWMH: deep-only WMH pattern in which WMHs are mainly located in the corticomedullary junction or deep white matter, accompanied by little or no periventricular WMH, dpWMH: WMH pattern that is commonly seen in individuals with cerebral small vessel disease, where main periventricular WMH with or without deep WMH is accompanied by one or more lacunes, WM, white matter.

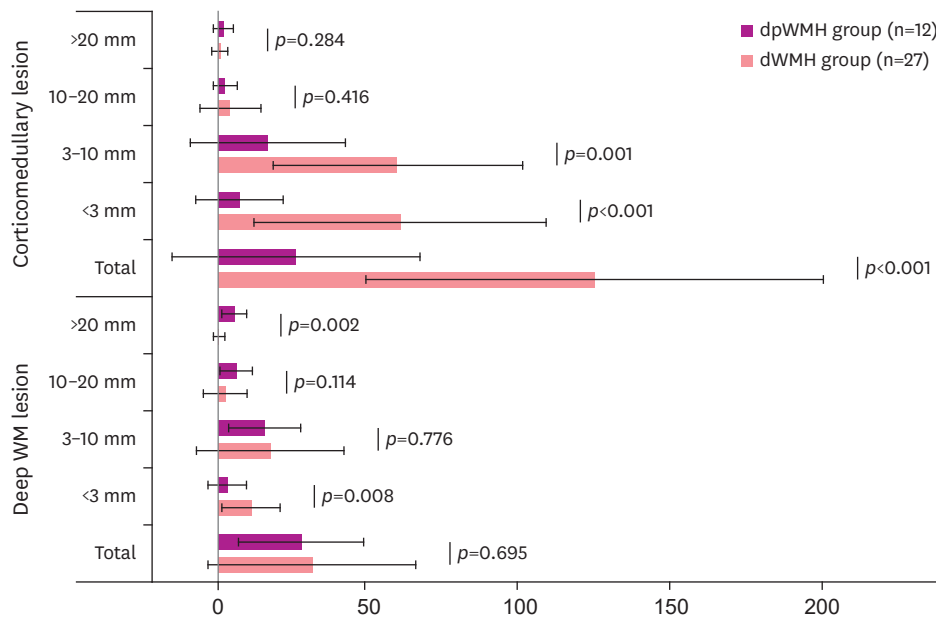


Fig. 3. Comparison of WMH distribution according to lesion size between the dWMH and dpWMH groups. The figure demonstrates that, in terms of deep white matter lesions, the number of small lesions (<3 mm) was higher in the dWMH than the dpWMH group, whereas the number of large lesions (>20 mm) was lower in the dWMH than the dpWMH group. In terms of corticomedullary lesions, the total number of lesions was higher in the dWMH than the dpWMH group, especially the number of small lesions was higher in the dWMH than the dpWMH group.

WMH: white matter hyperintensity, dWMH: deep-only WMH pattern in which WMHs are mainly located in the corticomedullary junction or deep white matter, accompanied by little or no periventricular WMH, dpWMH: WMH pattern that is commonly seen in individuals with cerebral small vessel disease, where main periventricular WMH with or without deep WMH is accompanied by one or more lacunes.

Comparison of shunt frequency between the dWMH and dpWMH groups

The dWMH group showed higher positivity in the agitated saline study than the dpWMH group (81.5% vs. 33.3%, $p=0.003$). The mean shunt grade of the dWMH group (1.8 ± 1.2) was significantly greater than that of the dpWMH group (0.5 ± 0.9) ($p=0.003$). All dpWMH individuals with positive saline tests belonged to Grade I or II, whereas 27.3% (6/22) of dWMH individuals with positive saline tests belonged to the large R-L shunt category (Grade III or IV). Of the 22 participants in the dWMH group who showed positivity in the agitated saline shunt study, four had extracardiac shunts. In the dpWMH group, of the four patients who showed positivity, two had extracardiac shunts (Table 3).

DISCUSSION

In the current study, we performed agitated saline contrast echocardiography in dpWMH and dWMH groups and examined whether the two groups differed in terms of shunt frequency. The dWMH group displayed higher positivity compared to the dpWMH group in the agitated saline studies. Among the 27 participants in the dWMH group, 18 had cardiac shunts, and four had extracardiac shunts. Among the 12 participants in the dpWMH group, two had cardiac shunts, and two had extracardiac shunts. Our findings suggest that dWMH patterns based on MRI may be associated with embolic etiologies, such as cardiac/extracardiac shunts, rather than small-vessel disease caused by atherosclerosis. In addition, the participants in the dWMH group had fewer vascular risk factors and were younger than those in the dpWMH group. The results of this study indicate that the dWMH pattern identified in FLAIR images represents embolic etiologies, which have not been comprehensively studied to date.

Deep WMH Distribution Suggests Embolic Etiology

Table 3. Comparison of shunt positivity between the dWMH and dpWMH groups

| Variables | dWMH group (n=27) | dpWMH group (n=12) | p-value |
|--------------------|-------------------|--------------------|---------|
| Saline shunt test | 22/27 (81.5) | 4/12 (33.3) | 0.003 |
| Intracardiac shunt | 18/22 (81.8) | 2/4 (50.0) | |
| Extracardiac shunt | 4/22 (18.2) | 2/4 (50.0) | |
| Shunt grade | 1.8±1.2 | 0.5±0.9 | 0.003 |
| 0 | 5 (18.5) | 8 (66.7) | |
| I | 4 (14.8) | 1 (8.3) | |
| II | 12 (44.4) | 3 (25) | |
| III | 4 (14.8) | 0 (0) | |
| IV | 2 (7.4) | 0 (0) | |

Values are presented as number (%) or mean ± standard deviation.

dWMH: deep-only WMH pattern in which WMHs are mainly located in the corticomedullary junction or deep white matter, accompanied by little or no periventricular WMH, dpWMH: WMH pattern that is commonly seen in individuals with cerebral small vessel disease, where main periventricular WMH with or without deep WMH is accompanied by one or more lacunes, WMH: white matter hyperintensity.

Previous studies reported that the distribution of WMH was associated with underlying etiologies. Typical CSVD is associated with vascular risk factors, predominantly pWMH.⁷ In contrast, a greater number of corticomedullary and deep WMH lesions can be identified in older patients with atrial fibrillation.³¹ Intracranial atherosclerotic plaques are also associated with deep WMH lesions, especially on the ipsilateral side.³² In addition, subcortical spots of WMH rather than peri-basal ganglia WMH may be seen in CAA.³³ In the present study, we excluded patients with atrial fibrillation and intracranial artery stenosis. We also ensured that our participants did not meet the Boston criteria for CAA.¹³

A few previous studies investigated the correlation between the distribution of WMH and the presence of PFO, but the results were inconsistent. One study reported that the radiologic findings of patients with PFO, one of the most common causes of cardiac embolism, showed a pattern similar to that of our dWMH group.⁹ However, another study reported that both deep and periventricular WMH was associated with the presence of PFO in Alzheimer’s disease (AD).³⁴ However, that study involving AD patients did not exclude participants who had intra/extracranial artery stenoses, previous stroke, or CAA. Again, our study strictly excluded embolic etiologies other than PFO and extracardiac shunts that could be detected in the agitated saline study. Such exclusions may have increased the robustness of the association between the dWMH pattern and the presence of cardiac/extracardiac shunts.

Among the 90 patients who underwent an agitated saline study with transthoracic echocardiography and brain MRI/MRA in the current study, 39 were categorized into two groups (dWMH and dpWMH groups) based on the distribution of WMH. Clinical characteristics and radiologic findings differed between the two groups. In terms of clinical characteristics, the participants in the dWMH group were younger and had higher MMSE scores than those in the dpWMH group (**Table 1**). In the post-hoc analysis, using linear regression, after pooling the dWMH and dpWMH groups, younger age was correlated with a lower presence of cardiovascular factors. These data are compatible with the risk of paradoxical embolism (RoPE) score, which is used to identify pathogenic versus incidental PFOs in patients with cryptogenic stroke.³⁵ Therefore, the white matter lesions in our dWMH group may be associated more with embolic causes such as PFOs rather than CSVD, which is closely linked to vascular risk factors such as hypertension, DM, and hyperlipidemia.

In terms of radiological findings, it is not surprising that the spatial distribution of WMH differed between the dWMH and dpWMH groups because we set the selection criteria to be predominantly located in deep areas, whereas the spatial distribution of WMH in the

dpWMH group was mainly located in the periventricular areas. However, it is noteworthy that the WMH lesions in the dWMH group were especially located in border zones or watershed areas, which are known to be selectively vulnerable to microembolic infarcts.³⁶ The deep white matter and corticomedullary junction in the border zone areas are considered to be the point at which the arteriole and collateral circulations end. Small emboli that may have escaped from the cardiac/extracardiac shunt can block small-diameter vessels and may eventually cause the WMH embolic pattern.³⁷ A marked difference in shunt frequency was observed when comparing the dWMH and dpWMH groups. The incidence of PFO in the general population or healthy individuals was reported to be quite high, approximately 30% in different studies, and varied by age (34.3% for 0 to 30 years, 25.4% for 40 to 80 years, and 20.2% for over 90 years).³⁸ The shunt positivity in our dpWMH group (33.3%) was comparable to the PFO positivity in the normal population in previous studies, whereas our dWMH group showed drastically higher shunt positivity (81.5%), indicating that dWMH patterns may be associated with embolic etiology rather than SVD caused by arteriosclerosis. According to previous studies, if the RoPE score is in the range of 9–10 in patients with cryptogenic embolic stroke, the frequency of PFO is 73% (95% confidence interval [CI], 66–79%), and the PFO attributable fraction is 88% (95% CI, 83–91%).¹² Therefore, the high positive rate (81.5%) in our study may be acceptable, albeit higher than expected, given that the mean RoPE score in the dWMH group was 6.0 ± 1.1 (min. 4–max. 8).

The association between the dWMH pattern and higher shunt positivity may have clinical implications. Although antiplatelet monotherapy is commonly administered to patients with CSVD, including lacunar infarcts, whether antiplatelet treatment for CSVD, especially at an asymptomatic disease stage, is beneficial remains controversial.^{39,40} In contrast, recent studies not only reported that PFO closure might be more effective in preventing recurrent stroke caused by paroxysmal embolism than medical therapy,^{41–44} but also suggested that patients with embolic etiologies, especially PFO, where intervention (PFO closure) is not possible, should be treated with oral anticoagulants (e.g., non-vitamin K antagonist oral anticoagulants, NOAC) rather than aspirin.^{41,42,45–48} Therefore, the dWMH pattern may help clinicians have a high index of suspicion for cardiac/extracardiac shunts and pursue in-depth investigations and more aggressive interventions, such as PFO closure or NOAC administration. Given that small, asymptomatic WMH lesions located in the deep WM or corticomedullary junction of young individuals (accompanied by few vascular risk factors) have been commonly overlooked in clinics to date, the findings of this study underscore the clinical significance of dWMH patterns observed in brain MRI.

This study had several limitations. First, there might have been selection bias because this study was based on a small number of participants retrospectively recruited from a single center. Therefore, prospective, multicenter, randomized studies involving larger sample sizes are warranted. Second, diagnostic uncertainty remains because transthoracic echocardiography with an agitated saline study is not the gold standard test to detect cardiac/extracardiac shunts.⁴⁹ Third, our data lack the confidence to suggest that the dWMH pattern was independent of an R-to-L shunt because age and vascular risk factors were not controlled when the WMH patterns of the two groups were compared. However, age and vascular risk factors in individuals with CSVD were reported to be positively correlated with the number of WMH lesions.^{50,51} Furthermore, in this study, individuals with the dWMH pattern had more corticomedullary and deep WMH lesions, although they were young and had few vascular risk factors. Therefore, the comparison of WMH lesions between the two groups without controlling for age and vascular risk factors may not entirely contradict our association

between the dWMH pattern and R-to-L shunt. Lastly, the occurrence of additional WMH according to antiplatelet or oral anticoagulant use or PFO closure should be investigated further in future studies.

The dWMH group with younger age and fewer cardiovascular risk factors showed more border-zone distributions and higher positivity in the agitated saline test than the dpWMH group. This indicates that corticomedullary or deep WMH distribution with minimal periventricular WMH may suggest embolic etiologies.

ACKNOWLEDGEMENTS

We would like to thank all the patients for their participation in the project.

SUPPLEMENTARY MATERIAL

Supplementary Fig. 1

Distribution of white matter lesions in the dWMH group. FLAIR images of the dWMH group show small, scattered white matter hyperintense lesions in the deep white matter and corticomedullary junction.

[Click here to view](#)

REFERENCES

1. Peppiatt CM, Howarth C, Mobbs P, Attwell D. Bidirectional control of CNS capillary diameter by pericytes. *Nature* 2006;443:700-704.
[PUBMED](#) | [CROSSREF](#)
2. Nishimura N, Rosidi NL, Iadecola C, Schaffer CB. Limitations of collateral flow after occlusion of a single cortical penetrating arteriole. *J Cereb Blood Flow Metab* 2010;30:1914-1927.
[PUBMED](#) | [CROSSREF](#)
3. Kang SH, Kim ME, Jang H, Kwon H, Lee H, Kim HJ, et al. Amyloid positivity in the Alzheimer/subcortical-vascular spectrum. *Neurology* 2021;96:e2201-e2211.
[PUBMED](#) | [CROSSREF](#)
4. Sarbu N, Shih RY, Jones RV, Horkayne-Szakaly I, Oleaga L, Smirniotopoulos JG. White matter diseases with radiologic-pathologic correlation. *Radiographics* 2016;36:1426-1447.
[PUBMED](#) | [CROSSREF](#)
5. Ye BS, Seo SW, Kim JH, Kim GH, Cho H, Noh Y, et al. Effects of amyloid and vascular markers on cognitive decline in subcortical vascular dementia. *Neurology* 2015;85:1687-1693.
[PUBMED](#) | [CROSSREF](#)
6. Lee JH, Kim SH, Kim GH, Seo SW, Park HK, Oh SJ, et al. Identification of pure subcortical vascular dementia using 11C-Pittsburgh compound B. *Neurology* 2011;77:18-25.
[PUBMED](#) | [CROSSREF](#)
7. Kim GH, Lee JH, Seo SW, Ye BS, Cho H, Kim HJ, et al. Seoul criteria for PiB(-) subcortical vascular dementia based on clinical and MRI variables. *Neurology* 2014;82:1529-1535.
[PUBMED](#) | [CROSSREF](#)
8. Griffanti L, Jenkinson M, Suri S, Zsoldos E, Mahmood A, Filippini N, et al. Classification and characterization of periventricular and deep white matter hyperintensities on MRI: a study in older adults. *Neuroimage* 2018;170:174-181.
[PUBMED](#) | [CROSSREF](#)

9. Bang OY, Lee MJ, Ryoo S, Kim SJ, Kim JW. Patent foramen ovale and stroke—current status. *J Stroke* 2015;17:229-237.
[PUBMED](#) | [CROSSREF](#)
10. Kim BJ, Sohn H, Sun BJ, Song JK, Kang DW, Kim JS, et al. Imaging characteristics of ischemic strokes related to patent foramen ovale. *Stroke* 2013;44:3350-3356.
[PUBMED](#) | [CROSSREF](#)
11. Boutet C, Rouffiange-Leclair L, Garnier P, Quenet S, Delsart D, Varvat J, et al. Brain magnetic resonance imaging findings in cryptogenic stroke patients under 60 years with patent foramen ovale. *Eur J Radiol* 2014;83:824-828.
[PUBMED](#) | [CROSSREF](#)
12. Kent DM, Ruthazer R, Weimar C, Mas JL, Serena J, Homma S, et al. An index to identify stroke-related vs incidental patent foramen ovale in cryptogenic stroke. *Neurology* 2013;81:619-625.
[PUBMED](#) | [CROSSREF](#)
13. Knudsen KA, Rosand J, Karluk D, Greenberg SM. Clinical diagnosis of cerebral amyloid angiopathy: validation of the Boston criteria. *Neurology* 2001;56:537-539.
[PUBMED](#) | [CROSSREF](#)
14. Kim S, Choi SH, Lee YM, Kim MJ, Kim YD, Kim JY, et al. Periventricular white matter hyperintensities and the risk of dementia: a CREDOS study. *Int Psychogeriatr* 2015;27:2069-2077.
[PUBMED](#) | [CROSSREF](#)
15. Ahn HJ, Chin J, Park A, Lee BH, Suh MK, Seo SW, et al. Seoul Neuropsychological Screening Battery-dementia version (SNSB-D): a useful tool for assessing and monitoring cognitive impairments in dementia patients. *J Korean Med Sci* 2010;25:1071-1076.
[PUBMED](#) | [CROSSREF](#)
16. Kang SH, Park YH, Lee D, Kim JP, Chin J, Ahn Y, et al. The cortical neuroanatomy related to specific neuropsychological deficits in Alzheimer's continuum. *Dement Neurocogn Disord* 2019;18:77-95.
[PUBMED](#) | [CROSSREF](#)
17. Attaran RR, Ata I, Kudithipudi V, Foster L, Sorrell VL. Protocol for optimal detection and exclusion of a patent foramen ovale using transthoracic echocardiography with agitated saline microbubbles. *Echocardiography* 2006;23:616-622.
[PUBMED](#) | [CROSSREF](#)
18. Saric M, Armour AC, Arnaout MS, Chaudhry FA, Grimm RA, Kronzon I, et al. Guidelines for the use of echocardiography in the evaluation of a cardiac source of embolism. *J Am Soc Echocardiogr* 2016;29:1-42.
[PUBMED](#) | [CROSSREF](#)
19. Rodrigues AC, Picard MH, Carbone A, Arruda AL, Flores T, Klohn J, et al. Importance of adequately performed Valsalva maneuver to detect patent foramen ovale during transesophageal echocardiography. *J Am Soc Echocardiogr* 2013;26:1337-1343.
[PUBMED](#) | [CROSSREF](#)
20. Carroll JD, Saver JL, Thaler DE, Smalling RW, Berry S, MacDonald LA, et al. Closure of patent foramen ovale versus medical therapy after cryptogenic stroke. *N Engl J Med* 2013;368:1092-1100.
[PUBMED](#) | [CROSSREF](#)
21. Clarke NR, Timperley J, Kelion AD, Banning AP. Transthoracic echocardiography using second harmonic imaging with Valsalva manoeuvre for the detection of right to left shunts. *Eur J Echocardiogr* 2004;5:176-181.
[PUBMED](#) | [CROSSREF](#)
22. Altaf N, Daniels L, Morgan PS, Lowe J, Gladman J, MacSweeney ST, et al. Cerebral white matter hyperintense lesions are associated with unstable carotid plaques. *Eur J Vasc Endovasc Surg* 2006;31:8-13.
[PUBMED](#) | [CROSSREF](#)
23. Inglese M, Bomsztyk E, Gonen O, Mannon LJ, Grossman RI, Rusinek H. Dilated perivascular spaces: hallmarks of mild traumatic brain injury. *AJNR Am J Neuroradiol* 2005;26:719-724.
[PUBMED](#)
24. Heier LA, Bauer CJ, Schwartz L, Zimmerman RD, Morgello S, Deck MD. Large Virchow-Robin spaces: MR-clinical correlation. *AJNR Am J Neuroradiol* 1989;10:929-936.
[PUBMED](#)
25. Medrano Martorell S, Cuadrado Blázquez M, García Figueredo D, González Ortiz S, Capellades Font J. Hyperintense punctiform images in the white matter: a diagnostic approach. *Radiologia (Madr)* 2012;54:321-335.
[PUBMED](#) | [CROSSREF](#)
26. Kim KW, MacFall JR, Payne ME. Classification of white matter lesions on magnetic resonance imaging in elderly persons. *Biol Psychiatry* 2008;64:273-280.
[PUBMED](#) | [CROSSREF](#)

27. Mahammedi A, Wang LL, Williamson BJ, Khatri P, Kissela B, Sawyer RP, et al. Small vessel disease, a marker of brain health: what the radiologist needs to know. *AJNR Am J Neuroradiol* 2022;43:650-660.
[PUBMED](#) | [CROSSREF](#)
28. Wardlaw JM, Smith EE, Biessels GJ, Cordonnier C, Fazekas F, Frayne R, et al. Neuroimaging standards for research into small vessel disease and its contribution to ageing and neurodegeneration. *Lancet Neurol* 2013;12:822-838.
[PUBMED](#) | [CROSSREF](#)
29. Greenberg SM, Vernooij MW, Cordonnier C, Viswanathan A, Al-Shahi Salman R, Warach S, et al. Cerebral microbleeds: a guide to detection and interpretation. *Lancet Neurol* 2009;8:165-174.
[PUBMED](#) | [CROSSREF](#)
30. Scheltens P, Leys D, Barkhof F, Huglo D, Weinstein HC, Vermersch P, et al. Atrophy of medial temporal lobes on MRI in "probable" Alzheimer's disease and normal ageing: diagnostic value and neuropsychological correlates. *J Neurol Neurosurg Psychiatry* 1992;55:967-972.
[PUBMED](#) | [CROSSREF](#)
31. Wiggins ME, Jones J, Tanner JJ, Schmalfluss I, Hossein Aalaei-Andabili S, Heilman KM, et al. Pilot investigation: older adults with atrial fibrillation demonstrate greater brain leukoaraiosis in infracortical and deep regions relative to non-atrial fibrillation peers. *Front Aging Neurosci* 2020;12:271.
[PUBMED](#) | [CROSSREF](#)
32. Ni L, Zhou F, Qing Z, Zhang X, Li M, Zhu B, et al. The asymmetry of white matter hyperintensity burden between hemispheres is associated with intracranial atherosclerotic plaque enhancement grade. *Front Aging Neurosci* 2020;12:163.
[PUBMED](#) | [CROSSREF](#)
33. Charidimou A, Boulouis G, Haley K, Auriel E, van Etten ES, Fotiadis P, et al. White matter hyperintensity patterns in cerebral amyloid angiopathy and hypertensive arteriopathy. *Neurology* 2016;86:505-511.
[PUBMED](#) | [CROSSREF](#)
34. Purandare N, Oude Voshaar RC, McCollum C, Jackson A, Burns A. Paradoxical embolisation and cerebral white matter lesions in dementia. *Br J Radiol* 2008;81:30-34.
[PUBMED](#) | [CROSSREF](#)
35. Strambo D, Sirimarco G, Nannoni S, Perlepe K, Ntaios G, Vemmos K, et al. Embolic stroke of undetermined source and patent foramen ovale: risk of paradoxical embolism score validation and atrial fibrillation prediction. *Stroke* 2021;52:1643-1652.
[PUBMED](#) | [CROSSREF](#)
36. Bergui M, Castagno D, D'Agata F, Cicerale A, Anselmino M, Maria Ferrio F, et al. Selective vulnerability of cortical border zone to microembolic infarct. *Stroke* 2015;46:1864-1869.
[PUBMED](#) | [CROSSREF](#)
37. Hwang TL, Close TP, Grego JM, Brannon WL, Gonzales F. Predilection of brain metastasis in gray and white matter junction and vascular border zones. *Cancer* 1996;77:1551-1555.
[PUBMED](#) | [CROSSREF](#)
38. Meissner I, Whisnant JP, Khandheria BK, Spittell PC, O'Fallon WM, Pascoe RD, et al. Prevalence of potential risk factors for stroke assessed by transesophageal echocardiography and carotid ultrasonography: the SPARC study. *Stroke Prevention: Assessment of Risk in a Community*. *Mayo Clin Proc* 1999;74:862-869.
[PUBMED](#) | [CROSSREF](#)
39. Smith EE, Saposnik G, Biessels GJ, Doubal FN, Fornage M, Gorelick PB, et al. Prevention of stroke in patients with silent cerebrovascular disease: a scientific statement for healthcare professionals from the American Heart Association/American Stroke Association. *Stroke* 2017;48:e44-e71.
[PUBMED](#) | [CROSSREF](#)
40. Yoon CW, Choi Y, Jeon S, Lee DH, Yoon BN, Park HK, et al. Is antiplatelet treatment effective at attenuating the progression of white matter hyperintensities? *PLoS One* 2017;12:e0176300.
[PUBMED](#) | [CROSSREF](#)
41. Mas JL, Derumeaux G, Guillon B, Massardier E, Hosseini H, Mechtouff L, et al. Patent foramen ovale closure or anticoagulation vs. antiplatelets after stroke. *N Engl J Med* 2017;377:1011-1021.
[PUBMED](#) | [CROSSREF](#)
42. Saver JL, Carroll JD, Thaler DE, Smalling RW, MacDonald LA, Marks DS, et al. Long-term outcomes of patent foramen ovale closure or medical therapy after stroke. *N Engl J Med* 2017;377:1022-1032.
[PUBMED](#) | [CROSSREF](#)
43. Søndergaard L, Kasner SE, Rhodes JF, Andersen G, Iversen HK, Nielsen-Kudsk JE, et al. Patent foramen ovale closure or antiplatelet therapy for cryptogenic stroke. *N Engl J Med* 2017;377:1033-1042.
[PUBMED](#) | [CROSSREF](#)

44. Lee PH, Song JK, Kim JS, Heo R, Lee S, Kim DH, et al. Cryptogenic stroke and high-risk patent foramen ovale: the DEFENSE-PFO trial. *J Am Coll Cardiol* 2018;71:2335-2342.
[PUBMED](#) | [CROSSREF](#)
45. Hart RG, Sharma M, Mundl H, Kasner SE, Bangdiwala SI, Berkowitz SD, et al. Rivaroxaban for stroke prevention after embolic stroke of undetermined source. *N Engl J Med* 2018;378:2191-2201.
[PUBMED](#) | [CROSSREF](#)
46. Hart RG, Diener HC, Coutts SB, Easton JD, Granger CB, O'Donnell MJ, et al. Embolic strokes of undetermined source: the case for a new clinical construct. *Lancet Neurol* 2014;13:429-438.
[PUBMED](#) | [CROSSREF](#)
47. Kasner SE, Swaminathan B, Lavados P, Sharma M, Muir K, Veltkamp R, et al. Rivaroxaban or aspirin for patent foramen ovale and embolic stroke of undetermined source: a prespecified subgroup analysis from the NAVIGATE ESUS trial. *Lancet Neurol* 2018;17:1053-1060.
[PUBMED](#) | [CROSSREF](#)
48. Carroll JD, Saver JL, Thaler DE, Smalling RW, Berry S, MacDonald LA, et al. Closure of patent foramen ovale versus medical therapy after cryptogenic stroke. *N Engl J Med* 2013;368:1092-1100.
[PUBMED](#) | [CROSSREF](#)
49. Ren P, Xie M. Diagnostic accuracy of transthoracic echocardiography for patent foramen ovale: a systematic review and meta-analysis. *Heart* 2012;98 Suppl 2:E304-E304.
[CROSSREF](#)
50. Wardlaw JM, Allerhand M, Doubal FN, Valdes Hernandez M, Morris Z, Gow AJ, et al. Vascular risk factors, large-artery atheroma, and brain white matter hyperintensities. *Neurology* 2014;82:1331-1338.
[PUBMED](#) | [CROSSREF](#)
51. Dickie DA, Ritchie SJ, Cox SR, Sakka E, Royle NA, Aribisala BS, et al. Vascular risk factors and progression of white matter hyperintensities in the Lothian Birth Cohort 1936. *Neurobiol Aging* 2016;42:116-123.
[PUBMED](#) | [CROSSREF](#)